Calculation of the rotation–vibration states of water up to dissociation

Hamse Y. Mussa and Jonathan Tennyson[a)]
Department of Physics and Astronomy, University College London, London WC1E 6BT, United Kingdom

(Received 21 July 1998; accepted 18 September 1998)

We present rotation–vibrational levels of water up to the dissociation limit using two recent, global potential energy surfaces. These calculations are performed using our recently developed discrete variable representation (DVR) based parallel code (PDVR3D), which runs on computers with massively parallel processors. Variational tests on the convergence of these results show convergence within 0.5 cm^{-1}. Analysis of the highest wave functions for the vibrational energy levels are also shown. Tests on previous calculations performed using conventional computers suggest that convergence for high-lying rotationally excited states is not as good as claimed.
 [S0021-9606(98)02548-3]

I. INTRODUCTION

Recently there has been a significant advance in the theoretical interpretation of rotation–vibration spectra of water, based on the use of first principles calculations.[1–3] Even with these new techniques there remain important challenges. For example, the recent analysis of the rotational spectrum of hot water recorded in sunspots resulted in the assignment of 1687 new transitions.[2,4] These transitions involve energy levels of water which extend halfway to dissociation. So far, however, this analysis has only covered the stronger features in the spectrum and about 85% of the observed lines remain unassigned. It is likely that these weaker transitions will involve states all the way to dissociation.

Performing rotation–vibration calculations which extend all the way to dissociation for a molecule such as water remains a difficult problem; it is the one which we address here. In order to meet this challenge we have adapted methods which have served well at low and medium energy for computers with massively parallel processors (MPP).[5,6] Whereas a number of groups have obtained converged energy levels (see, for example, Refs. 7–10), and, more rarely, wave functions, for the vibrational states of strongly bound molecules up to dissociation, we believe that this is the first study to also obtain all such levels for a rotationally excited molecule.

In the following section, we discuss the potential energy surfaces used in this study. Section III describes the formation of the Hamiltonian matrix and its diagonalization on MPP machines. Section IV presents results of accurate vibrational and rovibrational calculations on $H_2{}^{16}O$ up to dissociation. The article finishes with our concluding remarks.

II. POTENTIAL SURFACES

So far, calculations of rotation–vibration energies of water have concentrated on the ''spectroscopic'' energy region for which a number of accurate potentials, for example, Refs. 1, 11, and 12, are available. Global potential energy surfaces for water are generally less accurate. Recently, however, two reliable if still not spectroscopically accurate, global water potential energy surfaces have been reported. These are due to Varandas,[13] and Ho and co-workers.[14] Varandas' surface is fitted to experimental data while that of Ho *et al.* is based on *ab initio* calculations.

Varandas' surface consists of two parts, $V_1(\mathbf{R})$ and $V_2(\mathbf{R})$, linked by an energy switching procedure. The low energy behavior is governed by $V_2(\mathbf{R})$, which is the spectroscopically determined PJT1 (Polyansky–Jensen–Tennyson) potential,[11] while $V_1(\mathbf{R})$ is a modified form of the global many body expansion potential of Murrell and Carter.[15] The potential has a dissociation energy of $D_e = 43\,866$ cm^{-1}, which is reduced to $D_0 = 41\,088$ cm^{-1} when zero point energy effects are taken into account.

The Ho *et al.* surface, which we used for most of the calculations presented below, is a spline fit to a grid of 1280 *ab initio* points. The dissociation energy is slightly lower than for Varandas' potential with $D_e = 42\,886$ cm^{-1} and $D_0 = 40\,086$ cm^{-1}.

For purposes of comparison with previous calculations, some results are also presented for the spectroscopically determined PJT2 potential.[12] This surface is valid at higher energies than its predecessor (PJT1), but can only be considered reliable up to about halfway to dissociation.

III. THEORY

In this work we use Radau[16] coordinates. For molecules with a heavy central atom, such as water, these coordinates are similar to, but computationally more convenient than coordinates based on *OH* bond lengths and the $\hat{HOH}$ bond angle. For rotationally excited states we use a body-fixed axis system which places the *x* axis along the bisector of the Radau angle and the *z* axis perpendicular to this in the plane of the molecule.[17,18] This embedding places the *z* axis close to the *A* axis of the molecule. This means that for water the projection of the total angular momentum *J* on the *z* axis,

[a)]Electronic mail: j.tennyson@ucl.ac.uk

which we usually denote as k, is close to the approximate, but important rotational quantum number K_a.

We use the two-step variational approach of Tennyson and Sutcliffe[19] to treat rotationally excited states. The basic idea of the two-step approach is to first solve a series of problems for which k is assumed to be a good quantum number, i.e., the Coriolis coupling is neglected. There are $J+1$ $(k=0,1\ldots,J)$ such ''vibrational'' problems. The second step solves the fully coupled rovibrational problem using the eigenstates from the first step as a basis. The rapid convergence shown below (Table IV) for the second step arises as a result of the similarity between k and K_a.

The $J=0$ and the first step ''vibrational problem'' are solved using a discrete variable representation (DVR) in each coordinate based on a formulation which is well documented elsewhere.[18,20] In this formulation, the angular grids are based on the (associated) Legendre polynomials and the radial grids based on Morse oscillator-like functions. The exchange symmetry between the identical H atoms is introduced by symmetrizing the n_r radial grid points, α and β, by

$$|\alpha,\beta,q\rangle = 2^{-1/2}(1+\delta_{\alpha,\beta})^{-1/2}(|\alpha,\beta\rangle + (-1)^q|\beta,\alpha\rangle), \quad \alpha \geqslant \beta+q, \tag{1}$$

where q is a symmetry quantum number and takes the value 0 or 1. As discussed elsewhere,[3] this method of symmetrizing the grid is much more convenient for treating the extended range of bond lengths required for studies up to dissociation than the coordinate symmetrization employed by Light and co-workers.[21,22] The variational parameters of the Morse-like functions, r_e, ω_e, and D_e,[20] were optimized and set to $3.50a_0$, $0.0054E_h$, and $0.25E_h$, respectively. With one exception noted below, these parameters were used for all calculations reported here. All calculations were performed using atomic masses.

For water, our parallel version of the DVR3D program suite,[20] PDVR3D,[5,6] maps the vibrational problem onto an MPP machine by placing one of the n_θ active angular grid points onto each node. Some angular grid points, three in all the calculations presented below, closest to the *HHO* linear geometry are dropped from the calculation as required to avoid problems with singularities at this high energy geometry.[18] Each processor builds and diagonalizes the two-dimensional (2D) radial Hamiltonian. The lowest l eigenstates on each processor are selected and used as the basis for constructing its portion of the full three-dimensional (3D) Hamiltonian matrix. For reasons of load balancing, the same number of eigenvectors are retained for each angular grid point. This gives a final Hamiltonian size of $N=l\times n_\theta$. This algorithm is the sequential diagonalization and truncation approach.[23]

Bramley and Carrington[7] suggested that sequential diagonalization and truncation may be unnecessary. Their method, which has been adopted by a number of other groups, exploits iterative procedures to directly diagonalize the sparse but large uncontracted Hamiltonian matrix. Tests by Bramley and Carrington[8] found in practice that the procedure which is better is system dependent. For water, our tests found the Bramley–Carrington procedure to be much slower for water, even when an iterative diagonalizer was used in both methods.[5] In part, this was because we did not exploit symmetry in the nonsequential diagonalization and truncation calculations, as its inclusion leads to the loss of much of the simplicity of the Hamiltonian matrix. This simplicity is an important part of the efficiency of the procedure. As both methods gave very similar results, we only present calculations based on sequential diagonalization and truncation here.

As is usual for calculations on triatomics using standard computer architectures, it is the diagonalization of the final 3D Hamiltonian which dominates the computer time used. Parallel eigensolvers remain something of a problem. In previous work[5,6] we have tested full matrix diagonalizers such as PeIGS,[24] and the iterative PARPACK diagonalizer.[25] The results below were obtained using PARPACK.

Recently, Wu and Hayes[26] have presented results for the HO_2 molecule obtained on a MPP machine. They used an algorithm based on the iterative diagonalization of a Hamiltonian matrix which was obtained from sequential diagonalization and truncation but never explicitly constructed.

For calculations with $J>0$, the ''vibrational,'' i.e, $J=0$-like, calculations are repeated for each k between 0 and J. The h lowest eigenvectors from each k calculation are chosen as a basis for the second step of the calculation. For reasons of load balancing, h is kept independent of k, giving a final Hamiltonian of dimension $L=(k+1-p)\times h$, where the Wang parity is given by $(-1)^{(J+p)}$, $p=0,1$.

In a change from the algorithm used on conventional computers, matrix elements off-diagonal in k are calculated as part of the first step.[6] This procedure reduces both disk storage and I/O. These can become a bottle neck on the MPP machines used here on which disk space is limited and I/O is slow. The final Hamiltonians diagonalized here are relatively small and were diagonalized using PeIGS.[24]

IV. RESULTS

A. $J=0$

1. Convergence tests and energy levels

In order to establish the reliability of our results for a given potential we studied the convergence of our calculations with respect to increasing the size of the calculation. For $J=0$, it is necessary to consider three parameters: n_r, the number of radial DVR grid points, n_θ, the number of active angular DVR grid points, and N, the size of the final Hamiltonian matrix.

Table I shows the convergence of $q=0$ or even states near dissociation as a function of n_θ. To ensure variations arise solely from the variation in angular grid points, 120 solutions of the 2D ''radial'' Hamilton were used for each bending grid point. This means that N varies with n_θ, as shown in Table I. All the band origins below 38 000 cm^{-1} are converged to better than 0.1 cm^{-1}, whereas the states from 38 000 cm^{-1} up to the dissociation are converged to within 0.3 cm^{-1}.

Table II shows the effect of changing n_r, keeping N and n_θ fixed. Table II shows that the band origins converged to better than 0.2 cm^{-1}, apart from the final seven below disso-

TABLE I. Convergence of water ($J=0$, $p=0$, $q=0$, $n_r=50$) band origins, in cm^{-1}, up to dissociation as a function of n_θ, the angular primitive basis. N is the size of the Hamiltonian. $\Delta E(n_\theta - m_\theta)$ stands for the difference between calculation with n_θ basis and that with m_θ basis.

State	$n_\theta=48$ $N=5760$	Δ(64-48) 7680	Δ(80-64) 9600	Δ(96-80) 11 520
488	37 929.96	0.00	0.00	0.00
489	38 013.78	0.01	0.00	0.00
490	38 025.74	0.10	0.06	0.01
491	38 033.14	0.09	0.06	0.00
492	38 055.38	0.03	0.01	0.00
498	38 260.21	0.08	0.02	0.01
499	38 280.40	0.02	0.01	0.00
500	38 284.86	0.04	0.02	0.00
501	38 301.20	0.00	0.00	0.00
502	38 307.27	0.00	0.00	0.00
508	38 449.66	0.58	0.19	0.15
509	38 495.74	0.26	0.14	−0.02
510	38 542.71	0.00	0.00	0.00
511	38 552.84	0.02	0.01	0.00
512	38 565.05	0.00	0.00	0.00
518	38 645.91	0.07	0.05	−0.01
519	38 679.83	0.07	0.02	0.02
520	38 681.44	0.03	0.01	0.01
521	38 697.46	0.00	0.00	0.00
522	38 706.75	0.00	0.00	0.00
528	38 852.99	0.12	0.04	0.03
529	38 863.98	0.02	0.00	0.00
530	38 866.75	0.13	0.05	0.01
531	38 886.23	0.04	0.02	0.00
532	38 900.23	0.02	0.01	0.00
538	39 104.80	0.02	0.00	0.00
539	39 108.40	0.01	0.00	0.00
540	39 128.90	0.04	0.01	0.01
541	39 146.38	0.14	0.02	0.01
542	39 161.67	0.00	0.00	0.00
548	39 279.80	0.00	0.00	0.00
549	39 313.76	0.00	0.02	0.00
550	39 365.53	0.02	0.01	0.01
551	39 380.70	0.36	0.11	0.25
552	39 419.84	0.00	0.00	0.00
558	39 549.90	0.00	0.00	0.00
559	39 557.43	0.08	0.02	0.02
560	39 563.67	0.04	0.00	0.01
561	39 588.14	0.00	0.00	0.00
562	39 611.36	0.00	0.00	0.00
568	39 707.18	0.01	0.01	0.00
569	39 725.44	0.00	0.00	0.00
570	39 757.23	0.03	0.01	0.00
571	39 767.94	0.01	0.00	0.00
572	39 786.62	0.14	0.05	0.01
578	39 905.32	0.08	0.02	0.02
579	39 912.68	0.00	0.00	0.00
580	39 921.20	0.01	0.00	0.00
581	39 930.31	−0.10	−0.05	−0.03
582	39 942.99	0.12	0.05	−0.01
583	40 003.06	0.00	0.00	0.00
584	40 011.43	0.00	0.01	0.00
585	40 021.91	0.02	0.02	0.00
586	40 063.04	−0.05	−0.03	−0.02
587	40 076.29	−0.01	−0.01	0.00

TABLE II. Convergence of water ($J=0$, $p=0$, $q=0$, $n_\theta=64$, $N=7680$) band origins, in cm^{-1}, up to dissociation as a function of n_r, the number of radial grid points. $\Delta E(n_r - m_r)$ stands for the difference between calculation with n_r grid points and that with m_r.

State	$n_r=50$	Δ(60-50)	Δ(70-60)	Δ(78-70)
488	37 929.90	0.07	0.02	0.02
489	38 013.78	0.01	0.01	0.00
490	38 025.73	0.10	0.05	0.04
491	38 033.14	0.08	0.04	0.04
492	38 055.34	0.07	0.02	0.01
498	38 260.24	0.03	0.09	0.02
499	38 280.32	0.11	0.01	0.02
500	38 284.72	0.16	0.05	0.02
501	38 301.02	0.18	0.01	0.01
502	38 307.27	0.01	0.01	0.01
508	38 449.93	0.23	0.21	0.09
509	38 495.84	0.14	0.12	0.10
510	38 542.70	0.02	0.00	0.00
511	38 552.72	0.14	0.02	0.02
512	38 564.61	0.44	0.01	0.01
518	38 645.91	0.08	0.03	0.04
519	38 679.69	0.18	0.09	0.04
520	38 681.20	0.26	0.05	0.02
521	38 697.00	0.45	0.02	0.00
522	38 706.72	0.03	0.03	0.01
528	38 852.94	0.14	0.11	0.04
529	38 863.96	0.04	0.02	0.02
530	38 866.73	0.11	0.14	0.05
531	38 886.22	0.04	0.05	0.03
532	38 899.96	0.28	0.03	0.02
538	39 104.78	0.04	0.02	0.02
539	39 108.38	0.02	0.03	0.01
540	39 128.71	0.21	0.04	0.03
541	39 146.43	0.08	0.07	0.08
542	39 161.67	0.01	0.01	0.02
548	39 279.51	0.29	0.01	0.01
549	39 313.72	0.04	0.02	0.03
550	39 365.52	0.02	0.03	0.02
551	39 380.71	0.28	0.22	0.14
552	39 419.53	0.31	0.01	0.01
558	39 549.71	0.20	0.00	0.01
559	39 557.50	0.05	0.02	0.06
560	39 563.65	0.07	0.01	0.03
561	39 588.01	0.13	0.02	0.02
562	39 611.29	0.08	0.02	0.02
568	39 707.09	0.08	0.05	0.02
569	39 725.32	0.11	0.03	0.01
570	39 757.07	0.19	0.04	0.02
571	39 767.59	0.36	0.03	0.01
572	39 786.22	0.38	0.31	0.09
578	39 905.33	0.07	0.05	0.07
579	39 912.61	0.08	0.01	0.02
580	39 921.18	0.03	0.04	0.03
581	39 932.50	−2.07	−0.98	−0.39
582	39 943.04	0.05	0.09	0.08
583	40 003.14	−0.06	−0.09	−0.10
584	40 016.30	−4.21	−3.07	−1.49
585	40 025.76	−3.60	−0.77	−0.15
586	40 065.96	−2.64	−1.48	−0.70
587	40 077.03	−0.68	−0.30	−0.12

ciation, which show considerable sensitivity to the size of the radial grid selected. With the optimal Morse oscillator-like parameters given above, the grids with $n_r=50$, 60, 70 and 78 cover a region of the potential with $r=0.55-6.28a_o$, $0.26-6.56a_o$, $0.01-6.80a_o$ and $0.02-7.18a_o$, respectively. The range for the $n_r=78$ calculation is shifted to slightly larger r using $r_e=3.7a_o$. The relatively poor convergence of the last few states can be attributed to the long-range nature of the potential, which will support weakly bound, and dif-

TABLE III. Convergence of water ($J=0$, $p=0$, $q=0$, $n_\theta=64$ and $n_r=70$) band origins, in cm^{-1}, up to dissociation as a function of N, the size of the final Hamiltonian. $\Delta E(N\text{-}M)$ stands for the difference between calculation of Hamiltonian of order N and that of M.

State	$N=9600$	a	b	c
488	37 929.97	−0.09	−0.02	0.00
489	38 013.79	−0.03	0.00	0.00
490	38 025.84	−0.17	−0.08	−0.02
491	38 033.23	−0.15	−0.07	0.00
492	38 055.40	−0.07	−0.02	0.00
498	38 260.29	−0.27	−0.09	−0.02
499	38 280.42	−0.06	−0.02	0.00
500	38 284.90	−0.11	−0.04	0.00
501	38 301.20	−0.05	−0.02	0.00
502	38 307.27	−0.05	−0.01	0.00
508	38 450.23	−0.67	−0.39	−0.06
509	38 496.00	−0.46	−0.25	−0.04
510	38 542.71	−0.04	0.00	0.00
511	38 552.86	−0.08	−0.02	0.00
512	38 565.05	−0.04	0.00	0.00
518	38 645.98	−0.13	−0.04	−0.01
519	38 679.90	−0.29	−0.12	−0.02
520	38 681.47	−0.14	−0.04	−0.01
521	38 697.46	−0.04	0.00	0.00
522	38 706.75	−0.11	−0.02	0.00
528	38 853.11	−0.32	−0.12	−0.02
529	38 864.00	−0.09	−0.03	0.00
530	38 866.89	−0.38	−0.16	−0.03
531	38 886.27	−0.17	−0.06	−0.01
532	38 900.25	−0.11	−0.04	0.00
538	39 104.82	−0.11	−0.02	0.00
539	39 108.41	−0.09	−0.02	0.00
540	39 128.93	−0.16	−0.06	−0.02
541	39 146.52	−0.42	−0.16	−0.03
542	39 161.68	−0.10	−0.01	0.00
548	39 279.80	−0.07	0.00	0.00
549	39 313.77	−0.09	−0.04	0.00
550	39 365.55	−0.12	−0.04	−0.01
551	39 381.06	−0.81	−0.49	−0.07
552	39 419.84	−0.05	0.00	0.00
558	39 549.91	−0.06	−0.02	0.00
559	39 557.50	−0.35	−0.14	−0.02
560	39 563.71	−0.18	−0.05	−0.01
561	39 588.14	−0.09	−0.02	0.00
562	39 611.35	−0.10	−0.03	0.00
568	39 707.19	−0.11	−0.04	0.00
569	39 725.44	−0.10	−0.01	0.00
570	39 757.26	−0.16	−0.05	0.00
571	39 767.95	−0.11	−0.03	0.00
572	39 786.76	−0.64	−0.26	−0.04
578	39 905.40	−0.30	−0.10	−0.01
579	39 912.68	−0.12	−0.02	0.00
580	39 921.21	−0.16	−0.04	0.00
581	39 930.21	−0.06	−0.02	0.00
582	39 943.12	−0.40	−0.18	−0.02
583	40 003.06	−0.10	−0.01	0.00
584	40 011.43	−0.18	−0.06	−0.01
585	40 021.93	−0.38	−0.14	−0.02
586	40 062.99	−0.08	−0.02	0.00
587	40 076.27	−0.13	−0.03	0.00

[a] $\Delta E(10240-9600)$.
[b] $\Delta E(14720-10240)$.
[c] $\Delta E(17280-14720)$.

fuse states. We made no special efforts to converge these states.

Table III shows the convergence as a function of Hamiltonian size N. Our largest calculation converges all band origins to within 0.1 cm^{-1} with respect to increasing N. Our tests show that, with the exception of the final seven states, our calculations are converged to 0.5 cm^{-1} or better.

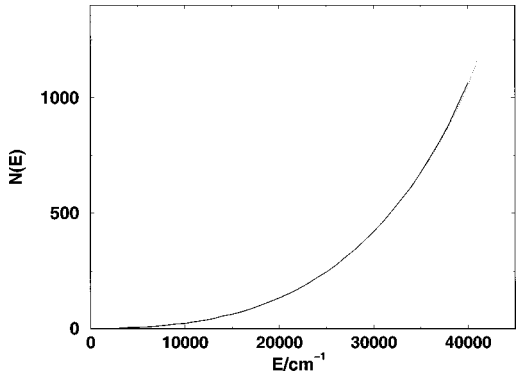

FIG. 1. Cumulative sum of energy levels up to an energy E, $N(E)$, as a function of energy for both Ho *et al.* (solid line) and Varandas potentials (dotted line).

In addition to the convergence, a close look at the tables shows different behavior of the DVR representation. Table III shows that the convergence is coming from above, which suggests the solution is variational. However, convergence in Table I implies the opposite; that convergence is mainly from below. Convergence in Table II is from both above and below. This behavior is just a reflection of the near-variational form of the DVR representation as discussed by Wei.[27]

We list only a selection of the highest even-parity levels to demonstrate convergence. Lower levels show no significant convergence error. Figure 1 presents the cumulative number $N(E)$ of energy levels up to an energy E, as a function of energy for both Ho *et al.* and Varandas surfaces. A complete list of $J=0$ vibrational energy levels for both parities for both the Ho *et al.* and Varandas potential energy surfaces can be obtained from the EPAPS archive.[28] These levels were obtained using $n_r=70$, $n_\theta=64$ and $N=17\,280$. For $J=0$, the Ho *et al.* surface supports 1076 states, whereas the Varandas surface supports 1169 states. Of course, our calculation will generally give a lower bound to the actual number of states supported by each potential. In particular, and as discussed below, it is likely that, for $J=0$, there are further very diffuse and weakly bound states which extend outside the range of our integration grid.

2. Wave functions

A wave function provides all the knowable information about a state. One way of assessing this information is to try to inspect its nodal structure visually.

To examine the wave function unambiguously it is necessary to inspect it fully, but in practice one cannot view more than two dimensions at a time. Examining 2D cuts by fixing one coordinate is the normal approach. Care must be taken as this procedure can be misleading because the apparent nodal structure depends on the coordinates used and on the particular cut taken. We have inspected many of the

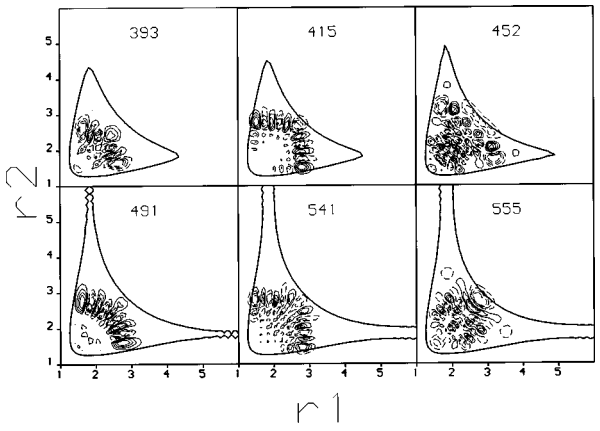

FIG. 2. Even-parity ($q=0$) non-local-mode wave functions of water plotted in Radau coordinates: r_1 vs r_2 in a_0 for a fixed angle $\theta=105.14°$. Solid and broken contours indicate positive and negative amplitude, respectively, and are placed at 16%, 32%, 48%, and 64% of the maximum amplitude. The solid line enclosing each state indicates the classical turning point for that state.

wave functions including a systematic study of the 200 highest even-parity states given by the Ho *et al.* potential. It is only possible to present a few of these here.

More than 75% of the highest 200 wave functions were found to be irregular with no readily identifiable nodal structure. The most common regular states are those showing local mode-type motion. However, even at these high energies quite a few states show clear normal mode behavior, as illustrated in Fig. 2. States 393, 491 and 541 show asymmetric normal-mode type in varying degrees, while states 452 and 555 can be considered as symmetric normal modes. However, state 415 shows a well-localized motion, which is neither local nor normal-mode type. It seems that the molecule is performing symmetric and asymmetric normal-mode-type motions, in which the two motions are perpendicular to each other. We also found several states which showed strong localization in the bending coordinate and could clearly be assigned as bending overtones.

Figures 3 and 4 give plots for the nine highest states. State 581 shows a combination of two local mode $O—H$ stretches. States 583 and 587 show simple local-mode local-

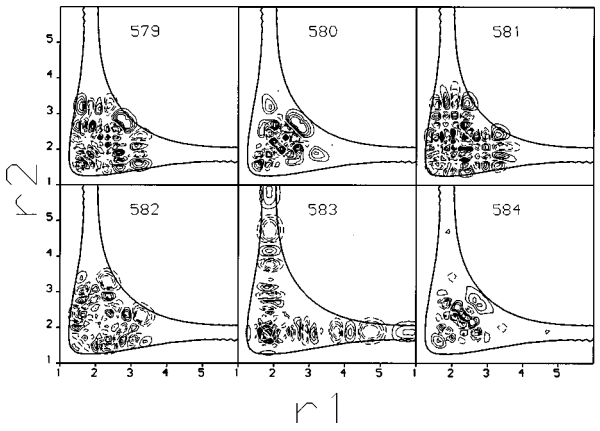

FIG. 3. Even-parity wave functions of water, at the dissociation limit. See Fig. 2 for details.

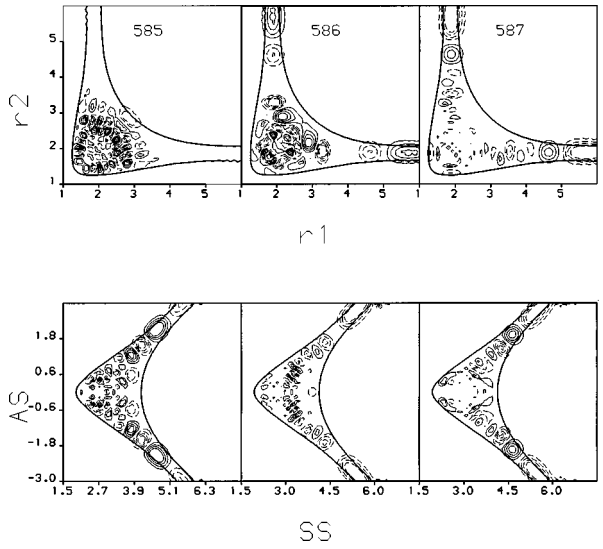

FIG. 4. The top panels show the highest three even-parity wave functions of water plotted in Radau coordinates with r_1 vs r_2 in a_0 for an angle $\theta=105.14°$. The bottom panels show the highest even-parity state of water plotted in symmetrized coordinates with *SS* (symmetric coordinate) versus *AS* (antisymmetric coordinate) in a_0 for, from left to right, $\theta=60°$, 90°, and 120°. Contours as in Fig. 2.

ization. State 587 is the highest even-parity state we found. For this state we present plots in symmetrized coordinates at different angles as well. As the bottom panels of Fig. 4 show, the localization of this state as a local-mode state persists in these representations. This, and a number of other local-mode states, sample regions with very large r. It is these states which show the slowest convergence properties in our calculations. All the other states in Figs. 3 and 4 appear to be irregular.

From this small sample, it is clear that even at the brink of dissociation modes can be decoupled and most of the energy can be trapped completely in one degree of freedom.

B. Rotational excitation

Calculations of the rovibrational energy levels were performed for a number of values of the rotational quantum number J. In particular, studies at the dissociation limit for $J=2$ were performed using the ''vibrational'' basis functions obtained from first step calculations with $k=0$, 1 and 2, and $n_\theta=64$, $n_r=70$, $N=7680$. Convergence of the rovibrational energy levels was tested by varying h, the number of first step eigenstates. Table IV shows the convergence of the last 100 states below the dissociation limit for $J=2$, $q=0$, $p=0$. All the energy levels are converged to within at least 0.4 cm^{-1}. A full list of energies calculated with $h=1152$ is available from the EPAPS archive.[28]

It should be noted that the Hamiltonian matrix diagonalized in the second step of our calculation is considerably smaller than those treated in the first step. Diagonalization dominates the computer time usage for the first step, whereas construction of the off-diagonal blocks in the second step also uses significant computer time. The size of these blocks is independent of J and their number increases linearly with J. In practice we find that computer time for rotationally

TABLE IV. Energies in cm^{-1} relative to the $J=0$ ground state of water with $J=2$, $p=0$, $q=0$. Convergence is shown as a function of h, the number of basis functions used for each k block. The size of the final Hamiltonian is given by $L=(J+1)\times h$. $\Delta h(n-m)$ indicates the difference between the $h=n$ calculation and that of $h=m$.

State	$h=768$	a	b	c
1525	39 412.63	−0.20	−0.07	−0.03
1526	39 429.54	−0.58	−0.17	−0.06
1527	39 442.41	−0.18	−0.04	−0.02
1528	39 454.20	−2.79	−0.46	−0.31
1529	39 456.27	−0.80	−0.16	−0.08
1535	39 514.27	−1.05	−0.27	−0.13
1536	39 525.55	−0.35	−0.09	−0.05
1537	39 529.02	−0.98	−0.14	−0.07
1538	39 544.92	−1.00	−0.20	−0.08
1539	39 554.49	−0.21	−0.11	−0.03
1545	39 593.61	−0.96	−0.20	−0.11
1546	39 599.19	−2.11	−0.27	−0.13
1547	39 601.73	−0.41	−0.13	−0.05
1548	39 611.85	−1.28	−0.18	−0.12
1549	39 618.99	−0.67	−0.13	−0.05
1555	39 639.75	−0.80	−0.20	−0.07
1556	39 648.96	−0.41	−0.18	−0.06
1557	39 650.89	−0.41	−0.12	−0.04
1558	39 664.93	−0.14	−0.04	−0.02
1559	39 670.01	−0.98	−0.18	−0.09
1565	39 697.43	−0.44	−0.11	−0.05
1566	39 709.35	−1.38	−0.27	−0.11
1567	39 713.97	−0.48	−0.17	−0.06
1568	39 718.08	−0.15	−0.05	−0.02
1569	39 727.00	−0.22	−0.07	−0.03
1575	39 765.97	−0.90	−0.11	−0.04
1576	39 772.82	−1.66	−0.24	−0.13
1577	39 774.65	−1.31	−0.25	−0.13
1578	39 781.57	−0.73	−0.14	−0.08
1579	39 799.36	−0.66	−0.16	−0.08
1585	39 830.95	−1.59	−0.30	−0.16
1586	39 833.49	−1.95	−0.26	−0.15
1587	39 837.70	−0.31	−0.07	−0.03
1588	39 856.45	−0.84	−0.21	−0.09
1589	39 857.20	−0.76	−0.21	−0.09
1595	39 885.54	−0.99	−0.24	−0.12
1596	39 903.64	−0.52	−0.21	−0.09
1597	39 910.93	−0.96	−0.29	−0.10
1598	39 921.65	−2.89	−0.53	−0.36
1599	39 931.60	−0.24	−0.07	−0.03
1605	39 968.96	−1.89	−0.29	−0.10
1606	39 971.11	−0.46	−0.16	−0.06
1607	39 974.46	−0.94	−0.19	−0.09
1608	39 978.02	−0.76	−0.21	−0.11
1609	39 982.75	−0.33	−0.17	−0.05
1615	40 010.66	−1.59	−0.32	−0.11
1616	40 015.64	−0.08	−0.04	−0.01
1617	40 022.92	−0.96	−0.28	−0.09
1618	40 042.24	−0.78	−0.14	−0.07
1619	40 045.68	−0.55	−0.13	−0.05
1620	40 064.10	−0.25	−0.27	−0.07
1621	40 064.95	−0.88	−0.18	−0.08
1622	40 071.14	−3.21	−0.27	−0.14
1623	40 074.11	−0.27	−0.09	−0.03
1624	40 081.65	−0.73	−0.15	−0.05

[a] $\Delta h(896-768)$.
[b] $\Delta h(1024-896)$.
[c] $\Delta h(1152-1024)$.

TABLE V. Water $J=6$, $p=0$, $q=0$, term values in cm^{-1}. Given are our term values and the differences, Δ, between our and the VT2 calculations of Viti and Tennyson (Ref. 29).

State	This work	Δ
1001	27 255.95	−0.93
1002	27 264.10	−0.86
1003	27 269.13	−0.45
1004	27 271.13	−0.91
1005	27 297.39	−0.85
1021	27 403.61	−0.40
1022	27 433.74	−0.83
1023	27 446.62	−0.64
1024	27 451.12	−0.75
1025	27 453.21	−0.45
1041	27 598.09	−0.45
1042	27 608.83	−0.53
1043	27 610.67	−1.15
1044	27 611.72	−0.96
1045	27 621.69	−0.58
1061	27 785.17	−0.47
1062	27 793.58	−1.15
1063	27 799.06	−0.94
1064	27 799.90	−1.16
1065	27 807.57	−0.67
1081	27 934.26	−0.90
1082	27 941.51	−0.77
1083	27 956.26	−1.77
1084	27 965.14	−1.32
1085	27 972.57	−1.34
1101	28 098.51	−0.50
1102	28 114.63	−1.80
1103	28 119.74	−0.55
1104	28 121.09	−1.98
1105	28 132.59	−1.68
1121	28 267.10	−0.73
1122	28 274.35	−1.42
1123	28 279.58	−1.34
1124	28 283.30	−2.01
1125	28 291.14	−2.02
1141	28 433.68	−0.60
1142	28 437.40	−1.07
1143	28 440.36	−2.23
1144	28 455.88	−1.24
1145	28 456.71	−1.38
1161	28 640.39	−3.17
1162	28 641.87	−2.07
1163	28 647.94	−2.43
1164	28 652.86	−0.61
11 65	28 659.06	−1.97
1181	28 790.84	−1.43
1182	28 800.97	−1.91
1183	28 817.61	−0.72
1184	28 834.07	−1.92
1185	28 840.57	−2.42
1201	28 981.10	−1.18
1202	28 994.93	−1.59
1203	28 998.56	−1.78
1204	29 005.54	−2.48
1205	29 011.37	−1.00
1221	29 135.45	−2.30
1222	29 137.16	−2.21
1223	29 141.99	−0.81
1224	29 154.15	−1.70
1225	29 159.42	−2.57
1241	29 293.47	−2.63
1242	29 296.50	−1.52
1243	29 299.99	−2.33
1244	29 302.27	−3.84

TABLE V. (*Continued*.)

State	This work	Δ
1245	29 329.97	−0.74
1261	29 433.46	−3.13
1262	29 439.36	−5.02
1263	29 447.35	−0.98
1264	29 449.84	−1.86
1265	29 451.48	−2.37
1281	29 563.36	−0.91
1282	29 575.89	−2.41
1283	29 587.99	−2.55
1284	29 593.34	−3.72
1285	29 596.95	−0.85
1301	29 727.52	−1.02
1302	29 739.58	−3.55
1303	29 751.52	−5.59
1304	29 756.91	−3.61
1305	29 773.04	−1.27
1321	29 915.02	−1.66
1322	29 916.01	−2.51
1323	29 924.51	−3.97
1324	29 935.83	−3.71
1325	29 946.12	−3.64
1326	29 948.59	−3.51
1327	29 950.81	−4.11
1328	29 960.87	−4.62
1329	29 964.91	−4.36
1330	29 970.88	−3.50
1331	29 974.00	−2.91
1332	29 981.23	−2.86
1333	29 988.54	−7.07
1334	29 996.75	−2.82

excited states is given by approximately $2\times(J+1)$ times the cost of a $J=0$ calculation, meaning that such calculations only grow linearly with J.

To our knowledge this is the first attempt to get all the rovibrational states of any $J>0$ for water. To test previous calculations we have also performed calculations using the PJT2 potential[12] employed by Viti and Tennyson (VT) for constructing their VT2 water line list.[29] We have compared all the 1334 $J=6$, $p=0$, $q=0$ states which lie below 30 000 cm^{-1}, the limit of the VT2 study. Table V compares a selection of the last 334 states of both calculations. VT also used DVR3D[20] and a two-step procedure for rotational excitation. Their ''vibrational'' calculations used $n_r=40$, $n_\theta=40$ (all ''active''), and a maximum of $h=700$. For the final Hamiltonian, for which $L=2100$, basis functions were selected using an energy cutoff procedure. Our results are for $n_r=40$, $n_\theta=48$ (plus three inactive points), $h=704$, and hence, $L=4928$.

There are two noticeable differences between the two calculations. The first is a small, systematic difference between the calculations which increases slowly with energy. This difference is caused by the use of slightly different masses in the VT2 calculation. Above 27 000 cm^{-1}, many of the states have more marked differences with those of VT2 lying up to 8 cm^{-1} higher. This comparison shows that the VT2 results are not completely converged in this region. We note that the recent line list calculations by Partridge and Schwenke[1] showed convergence difficulties for rotationally excited states at even lower energies.[4]

V. CONCLUSIONS

In this paper we have reported rotation–vibration states of water at its dissociation limit. We have shown that by harnessing advances in computer power and methodology it is now possible to tackle and study this challenging problem. Indeed, for $J=0$ these calculations took less than half-an-hour wall-clock time on 64 nodes of a Cray-T3E MPP computer. This means that it is possible to repeat such calculations to test and even improve potential energy surfaces. The linear scaling with rotational excitation, which might not hold at very high J values, suggests that the systematic treatment of rotationally excited states at dissociation is also well within the present capabilities.

Calculations using PDVR3D have been performed on a number of triatomics other than water. These results will be presented elsewhere.

ACKNOWLEDGMENTS

The authors thank Stephen Gray for providing his results prior to publication. These calculations have been performed as part of the EPSRC ChemReact Computing Consortium, and the authors thank the consortium members, Cliff Noble, Robert Allan, and the staff at Edinburgh Parallel Computing Center and Daresbury Laboratory for their help during the project.

[1] H. Partridge and D. W. Schwenke, J. Chem. Phys. **106**, 4618 (1997).
[2] O. L. Polyansky, N. F. Zobov, J. Tennyson, S. Viti, P. F. Bernath, and L. Wallace, Science **277**, 346 (1997).
[3] O. L. Polyansky, J. Tennyson, and N. F. Zobov, Spectro. Chemica Acta A (in press).
[4] O. L. Polyansky, N. F. Zobov, J. Tennyson, S. Viti, P. F. Bernath, and L. Wallace, J. Mol. Spectrosc. **186**, 422 (1997).
[5] H. Y. Mussa, J. Tennyson, C. J. Noble, and R. J. Allan, Comput. Phys. Commun. **108**, 29 (1998).
[6] H. Y. Mussa, J. Tennyson, C. J. Noble, and R. J. Allan in *High performance Computing*, edited by R. J. Allan, A. D. Simpson, and D. A. Nicole (Plenum, New York, 1998).
[7] M. J. Bramley and T. Carrington, Jr., J. Chem. Phys. **99**, 8519 (1993).
[8] M. J. Bramley and T. Carrington, Jr., J. Chem. Phys. **101**, 8494 (1994).
[9] V. A. Mandelshtam and H. S. Taylor, J. Chem. Soc., Faraday Trans. **93**, 847 (1997).
[10] R. F. Salzgeber, V. Mandelshtam, Ch. Schlier, and H. S. Taylor, J. Chem. Phys. **109**, 937 (1998).
[11] O. L. Polyansky, P. Jensen, and J. Tennyson, J. Chem. Phys. **101**, 7651 (1994).
[12] O. L. Polyansky, P. Jensen, and J. Tennyson, J. Chem. Phys. **105**, 6490 (1996).
[13] A. J. C. Varandas, J. Chem. Phys. **105**, 3524 (1996).
[14] T.-S. Ho, T. Hollebeck, H. Rabitz, L. B. Harding, and G. Schatz, J. Chem. Phys. **105**, 10472 (1996).
[15] J. N. Murrel, S. Carter, S. C. Farantos, P. Huxley, and A. J. C. Varandas, *Molecular Potential Energy Functions* (Wiley, Chichester, 1984).
[16] B. R. Johnson and W. P. Reinhardt, J. Chem. Phys. **85**, 4538 (1986).
[17] B. T. Sutcliffe and J. Tennyson, Int. J. Quantum Chem. **39**, 183 (1991).
[18] J. Tennyson and B. T. Sutcliffe, Int. J. Quantum Chem. **42**, 941 (1992).
[19] J. Tennyson and B. T. Sutcliffe, Mol. Phys. **58**, 1067 (1986).
[20] J. Tennyson, J. R. Henderson, and N. G. Fulton, Comput. Phys. Commun. **86**, 175 (1995).
[21] R. M. Whitnell and J. C. Light, J. Chem. Phys. **89**, 3674 (1988).
[22] S. E. Choi and J. C. Light, J. Chem. Phys. **97**, 7031 (1992).

[23] Z. Bacic and J. C. Light, Annu. Rev. Phys. Chem. **40**, 469 (1989).
[24] G. Fann, D. Elwood, and R. J. Littlefield, PeIGS Parallel Eigensolver System, User Manual available via anonymous ftp from pnl.gov.
[25] R. Lehoucq, K. Maschhoff, D. Sorensen, and C. Yang, PARPACK, available from ftp://ftp.caam.rice.edu/pub/people/kristyn.
[26] X. T. Wu and E. F. Hayes, J. Chem. Phys. **107**, 2705 (1997).
[27] H. Wei, J. Chem. Phys. **106**, 6885 (1997).
[28] See AIP Document No. EPAPS: E-JCPSA6-109-025848 for files containing the full set of $J=0$ energy levels for the potentials of Ho *et al.* and Varandas, and $J=2, q=0, p=0$ energy levels for the potential of Ho *et al.* EPAPS document files may be retrieved free of charge from our FTP server (http://www.aip.org/epaps/epaps.html) or from ftp.aip.org in the directory /epaps/. For further information, email: paps@aip.org or fax 516-576-2223.
[29] S. Viti, Ph.D. thesis, University of London, 1997; S. Viti and J. Tennyson (unpublished).